Available online at www.sciencedirect.com
ScienceDirect
Applied Catalysis B: Environmental 78 (2008) 355–363
APPLIED CATALYSIS B: ENVIRONMENTAL
www.elsevier.com/locate/apcatb

Comparative study of MTBE photocatalytic degradation with TiO_2 and Cu-TiO_2

J. Araña [a,b,*], A. Peña Alonso [a,b], J.M. Doña Rodríguez [a,b], J.A. Herrera Melián [a,b], O. González Díaz [a,b], J. Pérez Peña [a,b]

[a] *Fotocatálisis y Electroquímica Aplicada al Medio-Ambiente (FEAM), Unidad Asociada al Instituto de Ciencia de Materiales de Sevilla, C.S.I.C CIDIA (Depto. de Química), Edificio del Parque Científico Tecnológico, Campus Universitario de Tafira, 35017 Las Palmas, Spain*
[b] *Universidad de Las Palmas de Gran Canaria, Spain*

Received 27 July 2007; received in revised form 10 September 2007; accepted 15 September 2007
Available online 21 September 2007

Abstract

The photocatalytic techniques have been widely applied to the treatment of wastewaters. However, this work introduces an innovative application of photocatalysis to the treatment in continuous of gaseous contaminants. Packed reactors with different lengths and a spiral one have been designed to study the photocatalytic degradation of methyl *tert*-butyl ether (MTBE), individual alcohols and mixtures with their corresponding aldehydes. These studies have been performed with TiO_2 (Degussa P-25) and TiO_2 doped with Cu (Cu-TiO_2). The results obtained have shown that these systems can degrade and mineralize the tested compounds, thus achieving the decontamination of their gaseous emissions. Additionally, the reactor with Cu-TiO_2 has been more efficient than that with TiO_2 at the degradation and mineralization of MTBE, being the photocatalytic behaviour of the former more easily altered by the presence of intermediates.

Additionally, it has been observed that reactor morphology plays an important role in degradation efficiency. The spiral reactor with Cu-TiO_2, in which the catalyst was thermally deposited on the inner walls, achieved the highest degradation and mineralization of MTBE.

The obtained results are particularly interesting as an alternative to reduce emissions of volatile organic compounds to the atmosphere.

Keywords: MTBE; Gas phase photocatalysis; Spiral reactor; Cu-TiO_2

1. Introduction

In the last decades, the environmental effects of gaseous emissions from industries and other human activities have encouraged the public opinion to demand the control and reduction of such pollution. Consequently, in 1997 the governments of 55 nations agreed, by means of the Kyoto Protocol to reduce the emissions of greenhouse gases by 5.2%. The goal was to reduce the overall emissions of six greenhouse gases—carbon dioxide, methane, nitrous oxide, hydrofluorides, perfluorocarbons and sulfur hexafluoride. Nonetheless, in addition to these pollutants there are other volatile organic compounds (VOCs) which exert a deleterious effect on human health and pose a threat to the environment. Methyl *tert*-butyl ether (MTBE), a fuel additive produced from natural gas can be included in this group. It has been used in gasoline at low levels since 1979 to replace tetraethyl lead to increase its octane rating and help prevent engine knocking. MTBE is a volatile, flammable and colourless liquid that is relatively soluble in water. It has been shown that MTBE exposure causes sickness, skin eruption, respiratory problems and diarrhoea. The Environmental Protection Agency of the United States of America (EPA) has concluded that available data are not adequate to estimate potential health risks of MTBE at low exposure levels in drinking water, but that the data support the conclusion that MTBE is a potential human carcinogen at high doses. MTBE often ends up in drinking water, negatively affecting its taste and odour, even at very low concentrations. Thus, efficient techniques for the elimination of MTBE from water and air must be developed.

* Corresponding author at: Fotocatálisis y Electroquímica Aplicada al Medio-Ambiente (FEAM), Unidad Asociada al Instituto de Ciencia de Materiales de Sevilla, C.S.I.C CIDIA (Depto. de Química), Edificio del Parque Científico Tecnológico, Campus Universitario de Tafira, 35017 Las Palmas, Spain.
Tel.: +34 928 45 72 99; fax: +34 928 45 72 99.
E-mail address: jaranaesp@hotmail.com (J. Araña).

0926-3373/$ – see front matter
doi:10.1016/j.apcatb.2007.09.023

Different methods have been developed for the treatment of VOCs such as biofilters [1–4], membranes, electron beam systems [5–7] or the more traditional use of activated carbon, calcareous stone beds or modified minerals [8,9]. However, most of these techniques have important drawbacks that hamper their application at industrial scale. For instance, the use of biofilters is limited by the difficulty of pH control, the efficiency of electron beam methods is very low and adsorbents become saturated and deactivated by the presence of impurities.

The photocatalytic techniques have shown to be able to degrade and mineralize many organic wastes in water [10]. However, the elimination of the catalyst from aqueous phase is one of their main drawbacks. This is why many studies have been focused on the optimization of the process by depositing the catalyst (usually TiO_2) on different surfaces [11–13].

Many studies have been conducted to improve TiO_2 photocatalytic efficiency by means of the catalyst doping [14–19]. Nevertheless, success was achieved only in very specific processes. The catalyst's surface area and the alteration of surface hydroxyl group distribution can be cited among other negative effects of doping. One of the goals was to reduce electron-hole recombination by the metal reaction with the photogenerated electrons. However, it has been observed that the species reduced by their reaction with the photogenerated electrons were oxidised by the holes, inhibiting this way the formation of radicals [20].

The application of photocatalytic techniques in the treatment of gaseous wastes is not fully developed. Studies carried out in batch and continuous reactors have shown that these techniques can be very efficient if knowledge previously acquired with experiments in aqueous phase is applied.

In this work, the photocatalytic degradation of MTBE, individual alcohols and their mixtures with the corresponding aldehydes in gas phase has been studied with TiO_2 and TiO_2 doped with copper. Two types of reactors were used: catalyst packed reactors of different lengths and a spiral reactor with TiO_2 deposited on their inner walls by means of a simple thermal treatment.

2. Experimental

2.1. Catalyst preparation

TiO_2 was Degussa P-25 (80% anatase). Cu-TiO_2 was syntetized by impregnation of TiO_2 with aqueous solutions of $CuSO_4$, by an incipient wetness impregnation method [21] at 298 K as follows. The mixture (TiO_2 + metal) was stirred for 48 h. Later, water was evaporated by heating at 373 K over 24 h. Finally, the catalysts were calcined at 773 K for 5 h. Metallic precursor concentration was the one required to obtain 0.5% (w/w) of dopant. This catalyst has been charaterised in previous works by means of DRX analyses and FTIR studies of the surface hydroxyl groups [22]. These studies have not shown anatase-rutile ratio changes but the reduction of H-bonded surface hydroxyl groups. The presence of copper oxydes gives this catalyst a deep brown colour that changed in shade during these experiments in gas phase [22,23]. Additionally, degradation studies of different dihydroxybenzenes and carboxylic acids [24,25] carried out with this catalyst have confirmed the presence of Cu^{2+} ions on the surface.

2.2. Experimental conditions

All the experiments were carried out in a continuous reactor device at 35 °C (Fig. 1). This system consists of a vessel containing a 2:1 (v/v) water-MTBE solution at pH 5. pH of this solution was regulated by adding dilluted sulfuric acid (Fluka 84721). This vessel is continuously air-bubbled at a flow rate of 10 cm^3/min. The resulting air containing water and MTBE or others mixtures vapours is introduced in one (system 1) or five (system 2) 15-cm long, 4-mm diameter cylindrical Pyrex glass reactors containing the catalyst. Only the outer portion of the catalyst in contact with the inner wall of the reactor is exposed to the light and hence will be reactive. In order to compare their catalytic activities, the reactor was filled up to the same height (10-cm) with both catalysts. Thus, similar contact times are obtained. This way, each reactor of systems 1 and 2 contained 0.15 g of catalyst (TiO_2 or Cu-TiO_2). It must also be stressed that the five reactors of system 2 have been adequatly placed to receive each one of them the same photonic flow as the reactor of system 1.

Additionally, these experiments were also carried out in a 140-cm long spiral Pyrex glass reactor with a diammeter of 4 mm (system 3, Fig. 1), being the catalyst deposited on its inner walls by means of thermal treatments at 373 K with 2 g/L TiO_2 or Cu-TiO_2 suspensions. This impregnation process lasted 72 h achieving a homogeneous covering of the inner surface of the reactor. The amount of catalyst deposited was 0.03 g, approximately. This system has shown to be very stable during all the experiments performed in this work, without any noticeable catalyst detachment. In addition to the experiments with this reactor as part of system 3, other essays were carried out by introducing a fluorescent tube providing the same photonic flow as that of the other experiments along the inner space of this reactor (system 4, Fig. 1). The goal of this study was to determine the effect of different incident radiation angles in this reactor. However, the obtained efficiency was the same as those of systems 3 and 4.

In addition to this, thermal-blank degradation experiments of MTBE and the alcohols with the reactors of the different systems were performed without light with and without the catalysts. No degradation was observed in any of these controls.

Furthermore, it must be indicated that 10 cm^3/min was selected as the appropiate flow rate to compare the effect of different residence times of the pollutant in the systems and achieve a laminar flow to favour a plug flow regime in the reactor.

2.3. Equipment

The exhaust gases were continuously analysed by means of a GC (Varian Star 3600) equipped with a gas injection valve and a FID detector to determine MTBE and its reaction products such as alcohols, aldehydes and carboxylic acids. Additionally, a

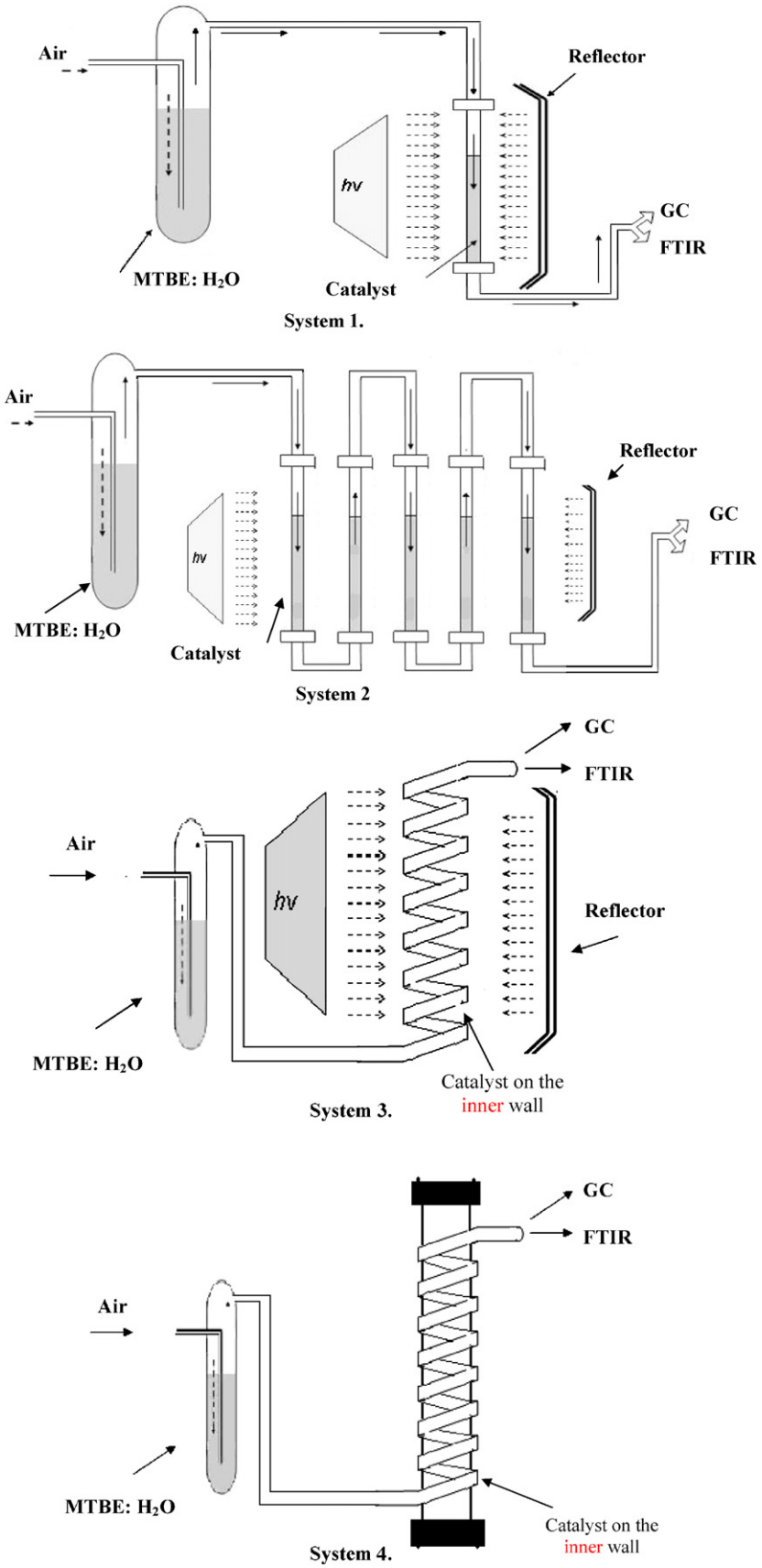

Fig. 1. Reaction systems.

TCD detector was used to determine CO_2. A catalytic chamber was employed to monitor intermediates on the catalyst surface by means of FTIR spectroscopy.

A 60-W Solarium Philips HB175 equipped with four 15-W Philips CLEO fluorescent tubes with emission spectrum from 300 to 400 nm (maximum at 365 nm) was used as UV source. The total incident light flux of this lamp is 2.45×10^{-8} photons mol cm^{-2} s^{-1}.

FTIR studies were carried out in a UNICAM model RS/1 FTIR spectrophotometer. Samples were placed in a cell with CaF_2 windows for spectra adquisition.

3. Results

3.1. Degradation studies with TiO_2

Fig. 2 shows MTBE concentration evolution during its photocatalytic degradation with TiO_2 in the system with only one reactor (Fig. 1, system 1). As can be observed, MTBE degradation was very low, only a 7% after 300 min of reaction. Formic acid and traces of CO_2 and *tert*-butyl alcohol were determined as MTBE degradation products.

Nevertheless, MTBE degradation in the system composed of 5 reactors (system 2) achieved 24% after 300 min of reaction (Fig. 3). Under these conditions the main products of reaction were *tert*-butyl alcohol, formic acid and CO_2 as product, being the concentrations of the former higher than those obtained with only one reactor.

In addition to this, MTBE photocatalytic degradation was studied in the spiral reactor (system 3) (Fig. 4). After 300 min the achieved degradation by this system was similar to that obtained by the reactor in series (Fig. 3). However, the main intermediate was formic acid, the same as with system 1. The presence of CO_2 and acetaldehyde was also detected in this reactor.

3.2. Degradation studies with Cu-TiO_2

Fig. 5 shows MTBE degradation results with Cu-TiO_2 in system 1. In this case, degradation was 14% after 300 min of reaction, two times higher than that obtained with TiO_2.

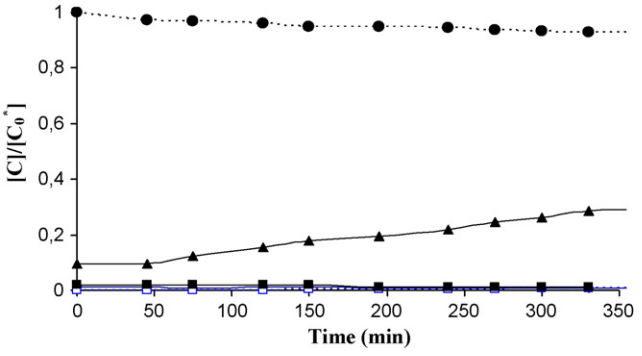

Fig. 2. Evolution of the concentrations of MTBE (●), reaction products (formic acid (▲), *tert*-butyl alcohol (□) and CO_2 (■)) during MTBE photocatalytic degradation in system 1. [C] = concentration of each compound. [C_0] = initial MTBE concentration.

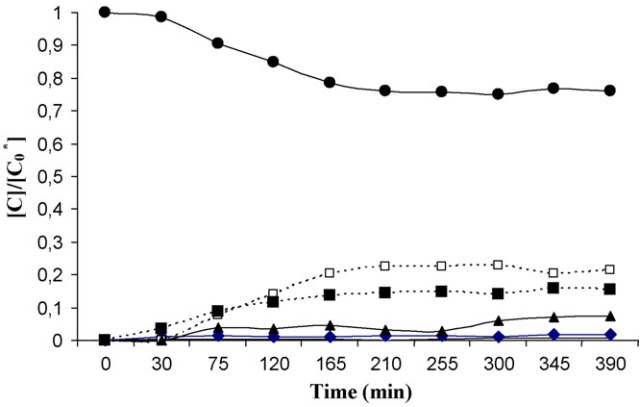

Fig. 3. Evolution of the concentrations of MTBE (●) reaction products (formic acid (▲), acetaldehyde (◆), *tert*-butyl alcohol (□) and CO_2 (■)) during MTBE degradation in system 2. [C] = concentration of each compound. [C_0] = initial concentration of MTBE.

Similarly to the observed with TiO_2, during the first minutes of reaction the main intermediate was formic acid. Nevertheless, at longer reaction times the concentration of formic acid was progressively reduced as that of CO_2 was increased. Moreover, in this study the concentration of acetaldehyde was lower than those of the other intermediates and remained almost constant during the experiment.

Furthermore, when Cu-TiO_2 was used in system 2, MTBE degradation achieved 50% after 300 min of reaction (Fig. 6). The main products were formic acid and CO_2. Lower concentrations of *tert*-butyl alcohol, acetaldehyde and acetic acid were also found. It must be stressed that the presence of formic acid and these last products was detected after the first 120 min of reaction.

Finally, the degradation of MTBE was studied in the spiral reactor (Fig. 7). The resulting MTBE degradation was 74% after 300 min of reaction, significantly higher than that obtained with the 5-reactor arrangement. Mineralization (≅56%) was also higher in this reactor. Formic acid and lower concentrations of acetaldehyde were also determined.

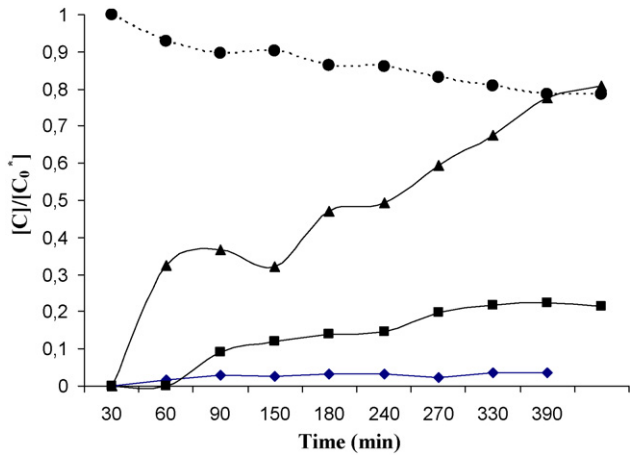

Fig. 4. Evolution of the concentrations of MTBE (●), reaction products (formic acid (▲), acetaldehyde (◆) and CO_2 (■)) during MTBE degradation in system 3. [C] = concentration of each compound. [C_0] = initial concentration of MTBE.

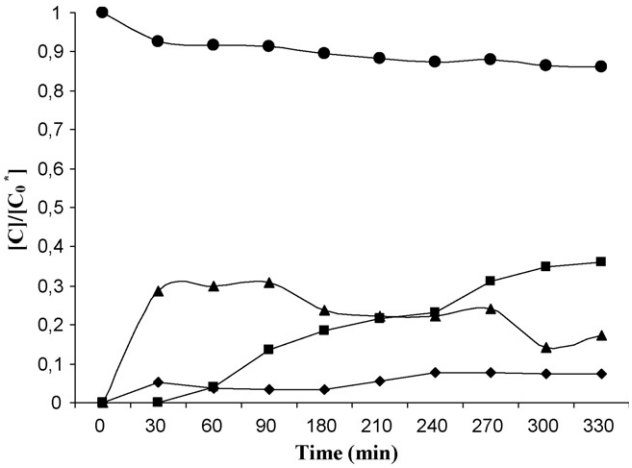

Fig. 5. Evolution of the concentrations of MTBE (●), reaction products (formic acid (▲), acetaldehyde (◆) and CO_2 (■)) during MTBE degradation in system 1 with Cu-TiO_2. [C] = concentration of each compound. [C_0] = initial concentration of MTBE.

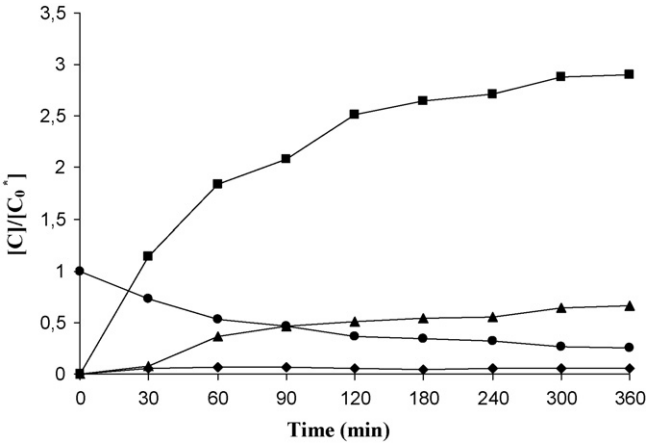

Fig. 7. Evolution of the concentrations of MTBE (●), intermediates (formic acid (▲), acetaldehyde (◆) and CO_2 (■)) during MTBE degradation in system 3 with Cu-TiO_2. [C] = concentration of each compound. [C_0] = initial concentration of MTBE.

Accordingly, it could be concluded that the spiral reactor is the most efficient of the studied systems at MTBE degradation and mineralization, as well. It must be remembered that in this case the photocatalysts was thermally deposited on the reactor's inner walls. In addition to this, Cu-TiO_2 showed a significantly higher efficiency than TiO_2.

As can be observed in Figs. 2–7, after the first 300 min of reaction with TiO_2 and Cu-TiO_2 all the systems achieved a steady state. These experiments continued for 48 h without any noticeable change.

3.3. Quantum efficiencies studies

Quantum efficiencies (ϕ) and apparent quantum efficiencies (ϕ_{app}) have been employed in many studies to compare the photocatalytic behaviour of different catalysts [26–32]. In the present work, apparent quantum efficiencies (ϕ_{app}) have been used to evaluate and compare the systems tested. Thus, ϕ_{app} has been defined as:

$$\phi_{app} = \frac{\text{moles of molecules of MTBE degraded per second and cm}^2}{\text{moles of incident photons per second and cm}^2}.$$

The moles of molecules of MTBE degraded per second and cm^2 has been calculated by multiplying the inflow rate by the conversion ratio obtained after 300 min of reaction (when degradation achieved a steady state) and dividing by the inner surface of each reactor. It has been also considered that in systems 1 and 2 only this section is photoactive. Results are shown in Table 1. As can be observed, apparent quantum efficiency of catalyst Cu-TiO_2 is higher than that of TiO_2 in all the reactors studied. Furthermore, ϕ_{app} becomes lower at higher reactor lengths. The apparent quantum efficiency reduction of system 2 with respect to system 1 with both catalysts is quite similar (31 and 28%, respectively). ϕ_{app} of system 3 with TiO_2 is 71% lower than of system 1. Additionally, ϕ_{app} of system 3 with Cu-TiO_2 is 57% lower than that of system 1. These remarkable differences between systems 3 and 1 can be attributed to the fact that, light penetration in the reactor of the former allows some inner layers and not only the outer one to be photoactive as suggested in the experimental section. In fact, if in the calculation of ϕ_{app} for systems 1 and 2, the photoactive surface is multiplied by 2, more similar values to those of system 3 are obtained.

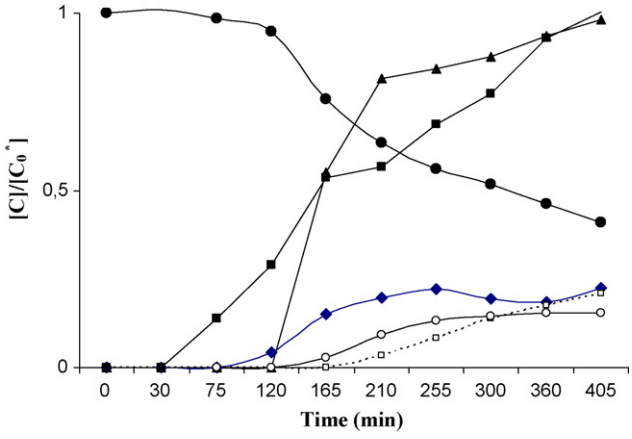

Fig. 6. Evolution of the concentrations of MTBE (●), intermediates (formic acid (▲), acetaldehyde (◆), *tert*-butyl alcohol (□), CO_2 (■) and acetic acid (○)) during MTBE degradation in system 2 with Cu-TiO_2. [C] = concentration of each compound. [C_0] = initial concentration of MTBE.

Table 1
Apparent quantum efficiencies for the degradation of MTBE as obtained after 300 min with TiO_2 and Cu-TiO_2 and for the different reaction systems

	ϕ_{app} (system 1)	ϕ_{app} (system 2)	ϕ_{app} (system 3)
TiO_2	0.0305	0.0209	0.0087
Cu-TiO_2	0.0610	0.0436	0.0260

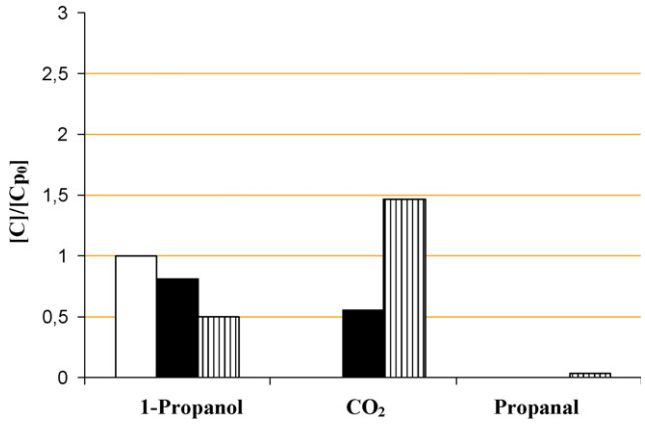

Fig. 8. Degradation of 1-propanol after 6 h of reaction (□, $t = 0$ min), (■, TiO_2) and (▥, Cu-TiO_2). Cp_o = initial concentration of 1-propanol. C = concentration of each compound after 6 h of reaction.

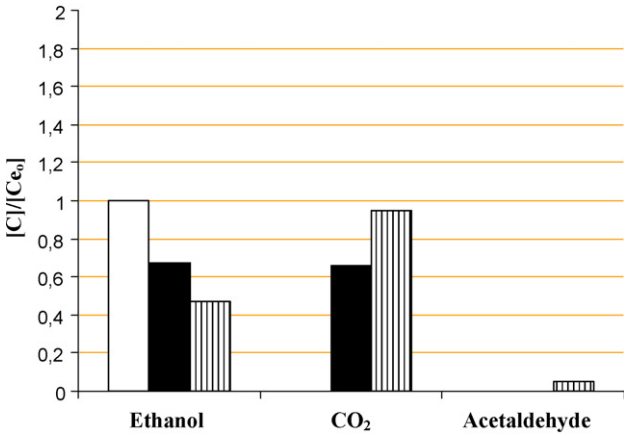

Fig. 10. Degradation of ethanol after 6 h of reaction (□, $t = 0$ min), (■, TiO_2) and (▥, Cu-TiO_2). Ce_o = initial concentration of ethanol. C = concentration of each compound after 6 h of reaction.

3.4. Photocatalytic degradation of alcohols and aldehydes

To check the photocatalytic efficiency of spiral reactor (system 3), the degradation of 1-propanol, ethanol and methanol and their 1:1 (v/v) mixtures with propanal, acetaldehyde and formaldehyde, respectively was studied. Previous studies with these alcohols and system 1 showed that Cu-TiO_2 was remarkably more efficient than TiO_2 [23]. These new experiments have been performed under the same conditions of concentration and flow than those of MTBE. Figs. 8–13 show the obtained results after 6 h of reaction.

As in the previous experiments, the highest mineralization of individual alcohols was achieved with Cu-TiO_2. The obtained mineralizations of 1-propanol, ethanol and methanol (Figs. 8, 10 and 12, respectively) were 50, 45 and 61%, respectively while 18, 32 and 42% with TiO_2. Additionally, in the experiments with the doped catalyst the corresponding aldehyde was detected although at very low concentrations (Figs. 8 and 10). This was not the case for the undoped TiO_2 for which no aldehydes were detected. Only formic acid was observed in the degradation of methanol (Fig. 12).

Moreover, in the experiments with equivolumetric mixtures of the alcohols and their corresponding aldehydes, the total mineralization of the aldehydes and a slight reduction of the photocatalytic degradation of the alcohols with respect to their individual experiments was observed with Cu-TiO_2. However, with TiO_2 a significant slowing down of the degradation of the alcohols in the mixture was obtained. These results seem to indicate that if TiO_2 is employed, the oxidation of these aldehydes is more favoured than that of the corresponding alcohols and that the presence of the latter clearly affects the degradation of the former.

The high reactivity of the aldehydes seems to be related with the reactor type employed. Thus, as observed in MTBE experiments with systems 1 and 2, the concentrations of aldehydes detected were higher than those measured in system 3.

4. FTIR studies

To interpret the possible mechanisms responsible for MTBE degradation, *in situ* FTIR studies of the catalyst surface have been performed. Fig. 14 shows MTBE reference spectrum

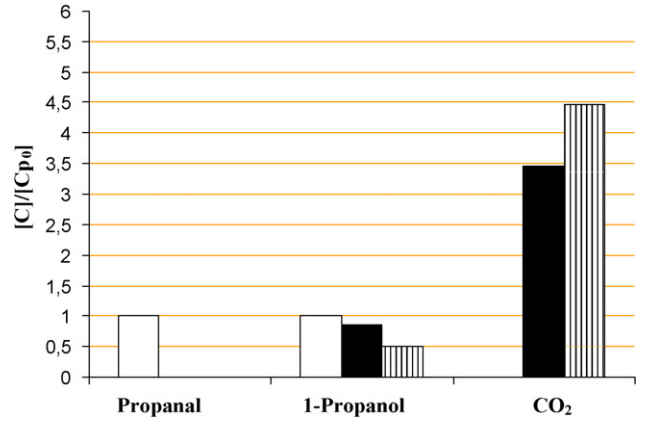

Fig. 9. Degradation of the mixture 1-propanol-propanal after 6 h of reaction (□, $t = 0$ min), (■, TiO_2) and (▥, Cu-TiO_2). Cp_o = initial concentration of 1-propanol or propanal. C = concentration of each compound after 6 h of reaction.

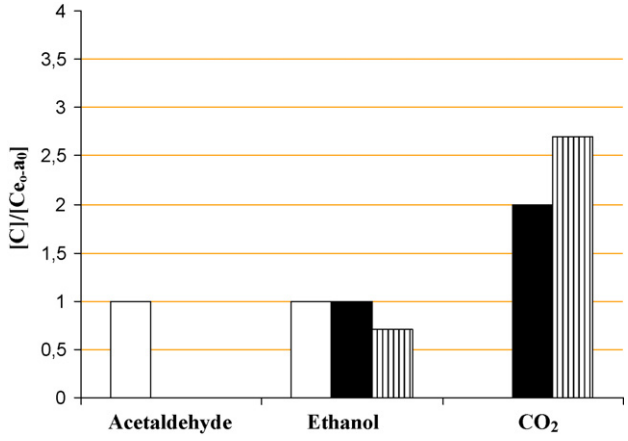

Fig. 11. Degradation of the mixture acetaldehyde–ethanol after 6 h of reaction (□, $t = 0$ min), (■, TiO_2) and (▥, Cu-TiO_2). Ce_o = initial concentration of ethanol or acetaldehyde. C = concentration of each compound after 6 h of reaction.

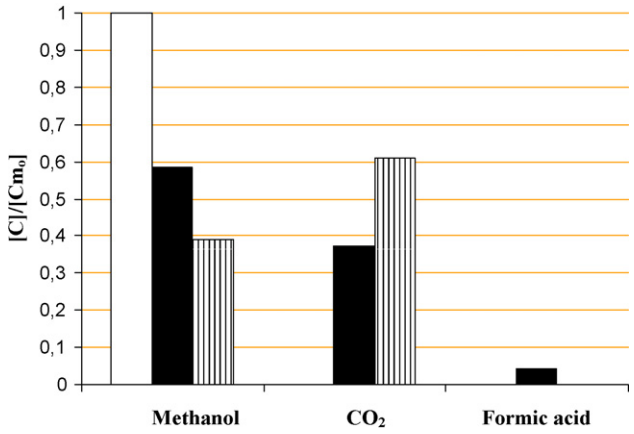

Fig. 12. Degradation methanol after 6 h of reaction (□, $t = 0$ min), (■, TiO_2) and (▥, Cu-TiO_2). Cm_o = initial concentration of methanol. C = concentration of each compound after 6 h of reaction.

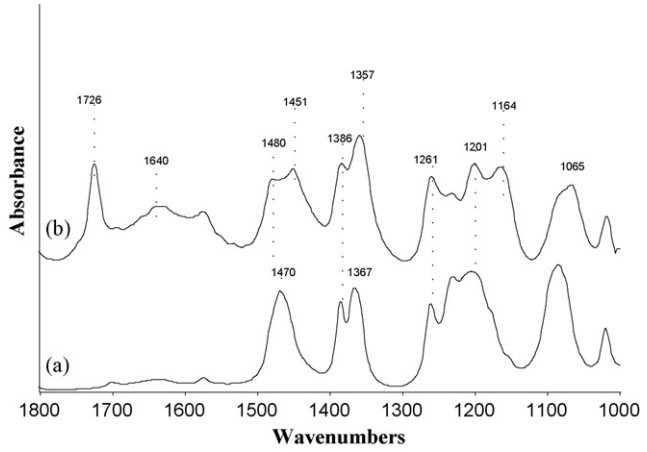

Fig. 14. FTIR reference spectrum of MTBE (a) and after 1 min of illumination in the presence of TiO_2 (b).

(Fig. 14a) and that obtained in the reactor (from catalytic chamber) after the first minute of reaction with the spiral reactor (Fig. 14b). The former has a band at 1726 cm^{-1} which was attributed ν (C=O) vibration and bands at 1480, 1451, 1386, 1357 and 1164 cm^{-1} ($\nu(CH_3)$) [33].

Fig. 15 shows the spectra obtained from TiO_2 surface after the 5, 10, 15 and 20 min of irradiation. The spectrum obtained after 5 min shows bands at 1582, 1370, 1199 and 1071 cm^{-1} which were attributed to formates ($HCOO^-$). However, at longer reaction times, several bands appearing at 1598, 1476 and 1430 cm^{-1} were attributed to acetates.

Fig. 16 shows the spectra from Cu-TiO_2 surface at different illumination times in the presence of MTBE. The spectrum obtained after 5 min with Cu-TiO_2 (Fig. 16a) is very similar to that from the gas phase after 1 min (Fig. 14b). Irradiating the sample during longer times resulted in the change of band intensities, although to a lesser extent than that observed with TiO_2. This means that the formation of acetate was not observed but low intensity bands at 1725–1700 and 1120–1000 cm^{-1}.

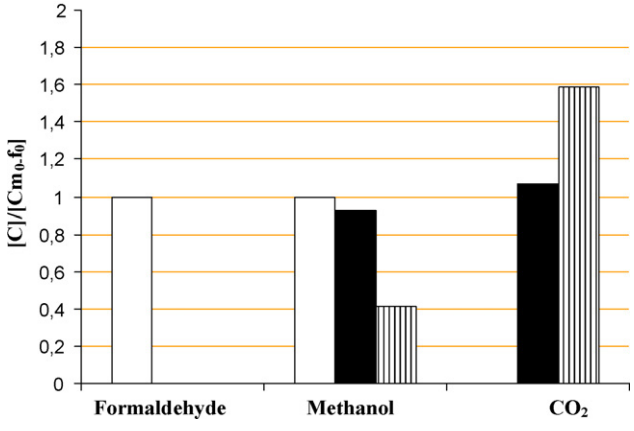

Fig. 13. Degradation of the mixture formaldehyde–methanol after 6 h of reaction (□, $t = 0$ min), (■, TiO_2) and (▥, Cu-TiO_2). Cm_o = initial concentration of methanol or formaldehyde. C = concentration of each compound after 6 h of reaction.

The obtained FTIR results in this work and others studies [34–41] suggest that MTBE degradation starts with reactions (1)–(3)

$$(CH_3)_3{-}C{-}O{-}CH_3 + {}^{\bullet}OH \rightarrow (CH_3)_3{-}C{-}O{-}CH_2{}^{\bullet} + H_2O \quad (1)$$

$$(CH_3)_3{-}C{-}O{-}CH_2{}^{\bullet} + O_2 \rightarrow (CH_3)_3{-}C{-}O{-}CH_2O_2{}^{\bullet} \quad (2)$$

$$2(CH_3)_3{-}C{-}O{-}CH_2O_2{}^{\bullet} \rightarrow 2(CH_3)_3{-}C{-}O{-}CHO + H_2O_2 \quad (3)$$

The following intermediate identified in this work and described for aqueous phase is *tert*-butyl alcohol [35,38,40,41] (reaction (4)). The formation of the following intermediates occurs mainly by direct oxidation with the holes (reactions (5)–(8)), although some of them can be formed by reaction with $^{\bullet}OH$ radicals.

$$(CH_3)_3{-}C{-}O{-}CHO + {}^{\bullet}OH \rightarrow (CH_3)_3{-}COH + HCOO^{\bullet} \quad (4)$$

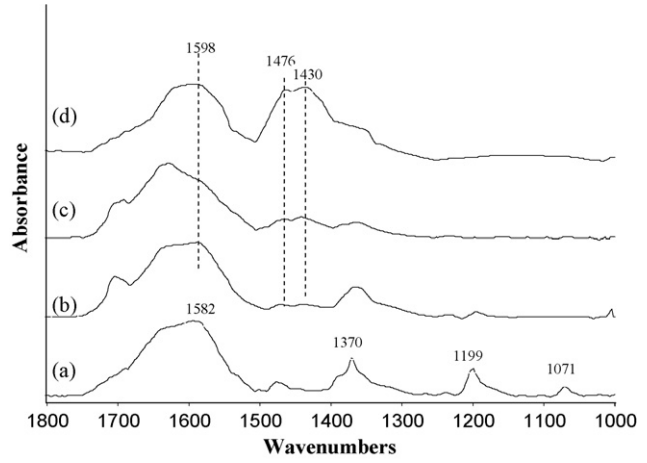

Fig. 15. FTIR spectra of MTBE adsorbed on TiO_2 after 5 (a), 10 (b), 15 (c) and 20 (d) minutes of illumination.

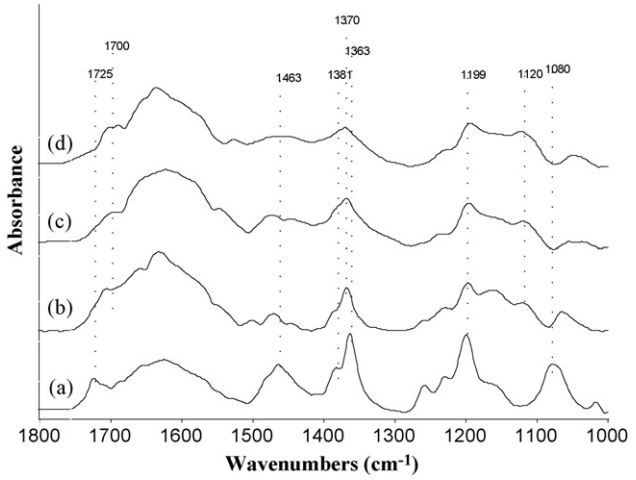

Fig. 16. FTIR spectra of MTBE adsorbed on Cu-TiO_2 surface after 5 (a), 10 (b), 15 (c) and 20 (d) minutes of illumination.

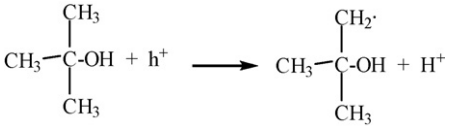

(5)

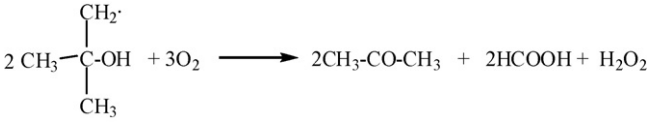

(6)

$$CH_3{-}CO{-}CH_3 + h^+ \rightarrow CH_3{-}CO{-}CH_2^{\bullet} + H^+ \quad (7)$$

$$CH_3{-}CO{-}CH_2^{\bullet} + O_2^{\bullet -} + H^+ \rightarrow CH_3{-}CHO + HCOOH \quad (8)$$

Superoxide radicals, $O_2^{\bullet -}$, are generated by means of O_2 reaction with photogenerated electrons and evolve to yield H_2O_2 (reactions (9)–(11)):

$$O_2 + e^- \rightarrow O_2^{\bullet -} \quad (9)$$

$$O_2^{\bullet -} + H^+ \rightarrow HO_2^{\bullet} \quad (10)$$

$$HO_2^{\bullet} + HO_2^{\bullet} \rightarrow H_2O_2 + O_2 \quad (11)$$

In addition to this, the degradation of the carboxylic acids is also described to happen by means of a Kolbe reaction, i.e., their direct reaction with holes instead of with $^{\bullet}OH$ radicals [15,42]:

$$R{-}COOH + h^+ \rightarrow R^{\bullet} + CO_2 + H^+ \quad (12)$$

The reaction of H_2O_2, generated in reactions (3) and (11), with the photogenerated electrons would increase $^{\bullet}OH$ radical concentration:

$$H_2O_2 + e^- \rightarrow {}^{\bullet}OH + OH^- \quad (13)$$

Considering the reduction potential for Cu^{2+}/Cu^+ (+0.17 V), CuO deposits present on TiO_2 surface can react with the photogenerated electrons through reaction (14). Cu^+ ions can be re-oxidised to Cu^{2+} by oxygen, H_2O_2 or other oxidising species present in the medium [43]:

$$Cu^{2+} + e^-_{cb} \rightarrow Cu^+ \quad (14)$$

$$Cu^+ \xrightarrow{(O_2, H_2O_2, \text{or other oxidants})} Cu^{2+} + e^- \quad (15)$$

The obtained results seem to indicate that these two reactions interfere with reactions (9) and (13) to diminish the formation of $^{\bullet}OH$ radicals. This could explain the different distribution of intermediates observed according to the catalyst used. Additionally, reaction of Cu^{2+} ions with the photogenerated electrons can slow down e^-/h^+ recombination. Thus, reactions in which holes intervene should be favoured and consequently mineralization enhanced.

In addition to this, another interesting result is the different MTBE intermediate distribution depending on the reactor system used. For instance, in the study with TiO_2 and system 1, which is the shortest one, the only intermediate detected was formic acid. However, in system 2 (five times longer than the former), *tert*-butyl alcohol and CO_2 were the most relevant products. This different behaviour could be attributed to the presence of formic acid in the exhaust gas of the first reactor of system 2 which it could be altering the catalyst surface and consequently its behaviour. This could also explain the lower ϕ_{app} obtained for system 2 with respect to system 1 (Table 1). Nevertheless, the intermediate distribution of the spiral reactor (system 3) is similar to that of system 1 although degradation is higher in latter. In this case, such higher degradation can be attributed to the larger contact surface of that system although ϕ_{app} is lower. This can be attributed, in addition to the above indicated higher radiation penetration in systems 1 and 2, to the effect of reaction products, as observed in system 2 in comparison to system 1.

The effect of the presence of a second compound on degradation and mineralization has been tested in the experiments performed with alcohols and their aldehydes. With TiO_2, the degradation of the alcohols was significantly slowed down by the presence of the aldehyde, being this effect not that strong with Cu-TiO_2. Additionally, FTIR studies have also revealed the different evolution of the photocatalytic process according to the catalyst used.

5. Conclusions

The reactors employed in this study have shown to be capable of transforming, diminishing or mineralizing gaseous emissions of MTBE, alcohols or aldehydes. The extent of the transformation depended on the dimensions of the reactor, i.e., residence time of the compound in the system.

The application of this type of reactors in workplaces in which VOCs are generated can reduce or eliminate their occupational hazards. The capability of using solar light as UV source makes their application simple, efficient and environmentally friendly.

This work has also shown that doping of TiO_2 with Cu remarkably improves photocatalytic activity and minimizes

deactivation. The reaction of Cu^{2+} ions deposited on the catalyst surface with the photogenerated electrons seems to be one the key process to explain the obtained photoactivity improvement.

ϕ_{app} results have shown that in addition to catalyst type, contact time and substrate to be degraded, reactor design is a key parameter to achieve efficient degradations in gas phase photocatalytic reactors. Additionally, reaction products can modify the catalyst behaviour depending on the reactor length and catalyst nature.

Acknowledgements

We are grateful to the Spanish Ministry of Science and Technology for providing research funding (CTQ2004-05734-CO2-01) and Ramón and Cajal Program 2003, to the Education Council of the Canarian Regional Government (Consejería de Educación del Gobierno Autónomo de Canarias) for further funding (PI2003/050).

References

[1] J.A. Mendoza, Ó.J. Prado, M.C. Veiga, C. Kennes, Water Res. 38 (2004) 404.
[2] M.A. Deshusses, Curr. Opin. Biotechnol. 8 (1997) 335.
[3] J.R. Kastner, D.N. Thompson, R.S. Cherry Kaster, Enzyme Microb. Technol. 24 (1999) 104.
[4] J. Martha Miller, D. Grant Allen, Chem. Eng. J. 113 (2005) 197.
[5] W. Reij Martine, J.T.F. Keurentjes, S. Hartmans, J. Biotechnol. 59 (1998) 155–167.
[6] M.S. Callén, M.T. de la Cruz, S. Marinov, R. Murillo, M. Stefanova, A.M. Mastral, Fuel Process. Technol. 88 (2007) 251.
[7] A.G. Chmielewski, E. Iller, Z. Zimek, M. Romanowski, K. Koperski, Rad. Phys. Chem. 45 (1995) 1029.
[8] W.Z. Khan, B.M. Gibbs, Energy 21 (2) (1996) 105.
[9] J.L. Venaruzzo, C. Volzone, M.L. Rueda, J. Ortiga, Micropor. Mesopor. Mater. 56 (2002) 73.
[10] O. Carp, C.L. Huisman, A. Reller, Prog. Solid State Chem. 32 (2004) 33.
[11] F.-L. Toma, G. Bertrand, S. Begin, C. Meunier, O. Barres, D. Klein, C. Coddet, Appl. Catal. B: Environ. 68 (2006) 74.
[12] F.-L. Toma, G. Bertrand, S.O. Chwa, D. Klein, H. Liao, C. Meunier, C. Coddet, Mater. Sci. Eng.: A 417 (2006) 56.
[13] J. Grzechulska, A.W. Morawski, Appl. Catal. B: Environ. 46 (2003) 415.
[14] G. Colón, M. Maicu, M.C. Hidalgo, J.A. Navío, Appl. Catal. B: Environ. 67 (2006) 41.
[15] J. Araña, O. González Díaz, J.M. Doña Rodríguez, J.A. Herrera Melián, C. Garriga i Cabo, J. Pérez Peña, M. Carmen Hidalgo, J.A. Navío-Santos, J. Mol. Catal. A: Chem. 197 (2003) 157.
[16] E. Piera, M.I. Tejedor-Tejedor, M.E. Zorn, M.A. Anderson, Appl. Catal. B: Environ. 46 (2003) 671.
[17] A. Di Paola, E. García-López, S. Ikeda, G. Marcì, B. Ohtani, L. Palmisano, Catal. Today 75 (2002) 87.
[18] D.W. Bahnemann, S.N. Kholuiskaya, R. Dillert, A.I. Kulak, A.I. Kokorin, Appl. Catal. B: Environ. 36 (2002) 161.
[19] J. Liqiang, F. Honggang, W. Baiqi, W. Dejun, X. Baifu, L. Shudan, S. Jiazhong, Appl. Catal. B: Environ. 62 (2006) 282.
[20] B. Xin, Z. Ren, P. Wang, J. Liu, L. Jing, H. Fu, Appl. Surf. Sci. 253 (2007) 4390.
[21] R.I. Bickley, J.S. Lees, R.J.D. Tilley, L. Palmisano, M. Schiavello, J. Chem. Soc., Faraday Trans. 88 (1992) 377.
[22] J. Araña, J.M. Doña-Rodríguez, O. González-Díaz, E. Tello Rendón, J.A. Herrera Melián, G. Colón, J.A. Navío, J. Pérez Peña, J. Mol. Catal. 215 (2004) 153.
[23] J. Araña, J.M. Doña-Rodríguez, J.A. Herrera Melián, E. Tello Rendón, O. González Díaz, J. Photochem. Photobiol. A: Chem. 174 (2005) 7.
[24] J. Araña, C. Garriga i Cabo, J.M. Doña-Rodríguez, O. González-Díaz, J.A. Herrera-Melián, J. Pérez-Peña, Appl. Surf. Sci. 239 (2004) 60.
[25] J. Araña, C. Fernández Rodríguez, J.M. Doña-Rodríguez, O. González-Díaz, J.A. Herrera-Melián, J. Pérez-Peña, Catal. Today 101 (2005) 26.
[26] Z. Jin, X. Zhang, Y. Li, S. Li, G. Lu, Catal. Commun. 8 (2007) 1267.
[27] H. Ibrahim, H. de Lasa, Chem. Eng. Sci. 58 (2003) 943.
[28] C. Wang, J. Rabani, D. Bahnemann, J. Dohrmann, J. Photochem. Photobiol. A: Chem. 148 (2002) 169.
[29] C. Wang, D.W. Bahneman, J.K. Dohrmann, Water Sci. Technol. 44 (2001) 278.
[30] A.N. Ökte, M.S. Resat, Y. Inel, J. Photochem. Photobiol. A: Chem. 134 (2000) 59.
[31] A. Salinaro, A.V. Emeline, J. Zhao, H. Hidaka, V.K. Ryabchuk, N. Serpone, Pure Appl. Chem. 7 (1999) 321.
[32] N. Serpone, J. Photochem. Photobiol. A: Chem. 104 (1997) 1.
[33] N.B. Colthup, L.H. Daly, S.E. Wiberley, Introduction to Infrared and Raman Spectroscopy, Academic Press, Inc., 1973.
[34] P.B.L. Chang, T.M. Young, Water Res. 34 (2000) 2233.
[35] M.I. Stefan, J. Mack, J.R. Bolton, Environ. Sci. Technol. 34 (2000) 650.
[36] A.A. Burbano, D.D. Dionysiou, T.L. Richardson, M.T. Suidan, J. Environ. Eng. 128 (2002) 799.
[37] C. Guillard, N. Charton, P. Pichat, Chemosphere 53 (2003) 469.
[38] R.D. Barreto, K.A. Gray, K. Anders, Water Res. 29 (1995) 1243.
[39] E. Sahle-Demessie, J. Enriquez, G. Gupta, Water Environ. Res. 7 (2002) 122.
[40] L.W. Kang, M.R. Hoffmann, Environ. Sci. Technol. 32 (1998) 3194.
[41] M. Bertelli, E. Selli, Appl. Catal. B: Environ. 52 (2004) 205.
[42] C. Guillard, J. Photochem. Photobiol. A: Chem. 135 (2000) 65.
[43] K. Chiang, R. Amal, T. Tran, Adv. Environ. Res. 6 (2002) 471.